Düzgünes, N., Hoekstra, D., Hong, K., & Papahadjopoulos, D. (1984) *FEBS Lett. 173*, 80–84.
Eytan, G. D., & Almary, T. (1983) *FEBS Lett. 156*, 29–32.
Gad, A. E. (1983) *Biochim. Biophys. Acta 728*, 377–382.
Gad, A. E., & Eytan, G. D. (1983) *Biochim. Biophys. Acta 727*, 170–176.
Gad, A. E., Silver, B. L., & Eytan, G. D. (1982) *Biochim. Biophys. Acta 690*, 124–132.
Hong, K., Düzgünes, N., & Papahadjopoulos, D. (1981) *J. Biol. Chem. 256*, 3641–3644.
Hong, K., Düzgünes, N., & Papahadjopoulos, D. (1982) *Biophys. J. 37*, 297–305.
Hong, K., Ekerdt, R., Bentz, J., Nir, S., & Papahadjopoulos, D. (1983) *Biophys. J. 41*, 31a.
Huang, C., & Mason, J. T. (1978) *Proc. Natl. Acad. Sci. U.S.A. 75*, 308–310.
Kagawa, Y., & Racker, E. (1971) *J. Biol. Chem. 246*, 5477–5487.
Liao, M. J., & Prestegard, J. H. (1979) *Biochim. Biophys. Acta. 550*, 157–173.
Lichtenberg, D., Freiere, E., Schmidt, C. F., Barenholz, Y., Felgner, P. L., & Thompson, T. E. (1981) *Biochemistry 20*, 3462–3647.
Nir, S. (1977) *Prog. Surg. Sci. 8*, 1–58.
Nir, S., Bentz, J., & Wilschut, J. (1980a) *Biochemistry 19*, 6030–6036.
Nir, S., Bentz, J., & Portis, A. (1980b) *Adv. Chem. 188*, 75–106.
Nir, S., Wilschut, J., & Bentz, J. (1982) *Biochim. Biophys. Acta 688*, 275–278.
Nir, S., Bentz, J., Wilschut, J., & Düzgünes, N. (1983a) *Prog. Surf. Sci. 13*, 1–124.
Nir, S., Düzgünes, N., & Bentz, J. (1983b) *Biochim. Biophys. Acta 735*, 160–172.
Ohki, S., Düzgünes, N., & Leonards, K. (1982) *Biochemistry 21*, 2127–2133.
Olson, F., Hunt, C. A., Szoka, F. C., Vail, W. J., & Papahadjopoulos, D. (1979) *Biochim. Biophys. Acta 557*, 9–23.
Papahadjopoulos, D., Vail, W. J., Newton, C., Nir, S., Jacobson, K., Poste, G., & Lazo, R. (1977) *Biochim. Biophys. Acta 465*, 579–598.
Portis, A., Newton, C., Pangborn, W., & Papahadjopoulos, D. (1979) *Biochemistry 18*, 780–790.
Schuber, F., Hong, K., Düzgünes, N., & Papahadjopoulos, D. (1983) *Biochemistry 22*, 6134–6140.
Sundler, R., & Papahadjopoulos, D. (1981) *Biochim. Biophys. Acta 649*, 743–750.
Sundler, R., Düzgünes, N., & Papahadjopoulos, D. (1981) *Biochim. Biophys. Acta 649*, 751–758.
Uster, P. S., & Deamer, D. W. (1985) *Biochemistry 24*, 1–8.
Vail, W. J., & Stollery, J. G. (1979) *Biochim. Biophys. Acta 551*, 74–84.
Wilschut, J., Düzgünes, N., Fraley, R., & Papahadjopoulos, D. (1980) *Biochemistry 19*, 6011–6021.
Wilschut, J., Düzgünes, N., & Papahadjopoulos, D. (1981) *Biochemistry 20*, 3126–3133.
Wilschut, J., Holsappel, M., & Jansen, R. (1982) *Biochim. Biophys. Acta 690*, 297–301.
Wilschut, J., Nir, S., Scholma, J., & Hoekstra, D. (1985) *Biochemistry 24*, 4630–4636.
Yemm, N. L., & Cocking, E. C. (1955) *Analyst (London) 80*, 209–223.
Young, T. M., & Young, J. D. (1984) *Biochim. Biophys. Acta 775*, 441–445.

Two Types of Hydrocarbon Chain Interdigitation in Sphingomyelin Bilayers†

I. W. Levin*
Laboratory of Chemical Physics, National Institute of Arthritis, Diabetes, and Digestive and Kidney Diseases, National Institutes of Health, Bethesda, Maryland 20205
T. E. Thompson, Y. Barenholz, and C. Huang*
Department of Biochemistry, University of Virginia School of Medicine, Charlottesville, Virginia 22908
Received April 11, 1985

ABSTRACT: Vibrational Raman spectroscopic experiments have been performed as a function of temperature on aqueous dispersions of synthetic DL-*erythro*-*N*-lignoceroylsphingosylphosphocholine [C(24):SPM], a racemic mixture of two highly asymmetric hydrocarbon chain length sphingomyelins. Raman spectral peak-height intensity ratios of vibrational transitions in the C–H stretching-mode region show that the C(24):SPM–H_2O system undergoes two thermal phase transitions centered at 48.5 and 54.5 °C. Vibrational data for fully hydrated C(24):SPM are compared to those of highly asymmetric phosphatidylcholine dispersions. The Raman data are consistent with the plausible model that the lower temperature transition can be ascribed to the conversion of a mixed interdigitated gel state (gel II) to a partially interdigitated gel state (gel I) and that the higher temperature transition corresponds to a gel I → liquid-crystalline phase transition. The observation of a mixed interdigitated gel state (gel II) at temperatures below 48.5 °C implies that biological membranes may have lipid domains in which some of the lipid hydrocarbon chains penetrate completely across the entire hydrocarbon width of the lipid bilayer.

Among the various choline-containing phospholipids present in eukaryotic biological membranes, sphingomyelin or *N*-acyl-sphingosylphosphocholine is a major component of most plasma membranes. The sphingomyelin isolated from plasma membranes is, in general, a mixutre of many molecular species with various fatty acyl chain moieties. Stearic, nervonic, lignoceric, and behenic acids constitute the major fatty acyl

†This work was supported by National Institutes of Health Grants GM-17452, GM-14628, and HL-17576.

0006-2960/85/0424-6282$01.50/0

groups (Barenholz & Thompson, 1980). It is interesting to note that the sphingosine moiety, which is common to virtually all sphingomyelins, contributes one hydrocarbon chain of 15 carbons to the molecule. Consequently, in most natural sphingomyelins the *N*-acyl chain contains substantially more methylene units than does the other hydrocarbon chain contributed by sphingosine. Each molecular species thus exhibits a marked hydrocarbon chain length asymmetry.

On the basis of X-ray diffraction and electron microscopic studies of dispersions of highly chain-length asymmetric saturated phosphatidylcholines such as C(18):C(10)PC[1] and C(18):C(12)PC, it has been proposed that, in the gel-state bilayer, these fully hydrated synthetic phospholipids adopt a mixed interdigitated chain packing, which is more ordered than the usual hydrated noninterdigitated bilayer (McIntosh et al., 1984; Hui et al., 1984). In the mixed interdigitated bilayer of gel-state phosphatidylcholines, the shorter *sn*-2 acyl chain is packed end to end with the *sn*-2 acyl chain of another lipid molecule in the opposing bilayer leaflet, while the longer *sn*-1 acyl chain from the two leaflets spans the entire hydrocarbon width of the bilayer. The mixed interdigitated gel bilayer is thus characterized by having the area per molecule at the lipid/water interface encompass three hydrocarbon chains, in contrast to the two hydrocarbon chains per lipid head group for phospholipids in noninterdigitated bilayers. Since most natural sphingomyelin molecules are chain-length asymmetric, one would expect to observe some manifestation of chain interdigitation in gel-state sphingomyelin lamellae. In this paper, we present Raman spectroscopic evidence to show that a fully hydrated synthetic spingomyelin with a lignoceroyl acyl group [C(24):SPM] undergoes two thermal phase transitions in the temperature range of 30–65 °C. The first or lower temperature transition is most likely a gel II → gel I transition with the mixed interdigitated phase as the more ordered gel II state and a partially interdigitated phase as the higher temperature gel I state. The second transition appears to correspond to a gel I → liquid-crystalline phase transition. Calormetric evidence for the existence of transitions in this temperature range has been reported previously for C(24):SPM dispersed in 50 mM KCl solution (Barenholz et al., 1976).

Experimental Procedures

Materials. DL-*erythro*-*N*-Lignoceroylsphingosylphosphocholine [C(24):SMP] was a gift from Professor D. Shapiro, Weizman Institute of Science, Rehovot, Israel. After further purification by silicic acid chromatography and precipitation from acetone, the lipid was first suspended in distilled water to form an aqueous dispersion with a lipid concentration of 20% (w/w). The lipid dispersion was micropipetted into a Kimex glass capillary tube (1.25-mm i.d.) and then hermetically sealed. After the capillary was spun in a bench-top clinical centrifuge at room temperature, the sample was incubated at 60 °C for 5 min and then allowed to anneal at 0 °C for a minimum of 1 month prior to use. This long incubation time was taken to ensure reproducible results.

Raman Spectroscopy. Vibrational Raman spectra were obtained with a Spex Ramalog 6 spectrometer equipped with holographic gratings and interfaced to a Nicolet NIC-1180 data acquisition system, as described previously (Huang et al, 1982). In general, Raman spectra were recorded at a scanning rate of 1 cm^{-1}/s with a laser excitation (514.5 nm) power of 200–220 mW at the sample. Temperature profiles were recorded in an ascending-temperature mode; the sample was heated in 2 °C increments with a 12-min equilibration time at each temperature prior to recording the spectrum. Three to four signal-averaged spectral scans were acquired at each temperature. Temperature profiles for the multilamellar phospholipid assemblies were constructed from the Raman spectral peak-height intensity ratios $I(2932\ cm^{-1})/I(2882\ cm^{-1})$ and $I(2847\ cm^{-1}/I(2882\ cm^{-1})$. Although the spectral peak frequencies shift slightly to higher values on increasing tempeature, we used the low-temperature gel-phase values for identifying vibrational transitions and intensity ratios. Neither spectral deconvolution nor contour smoothing procedures were applied.

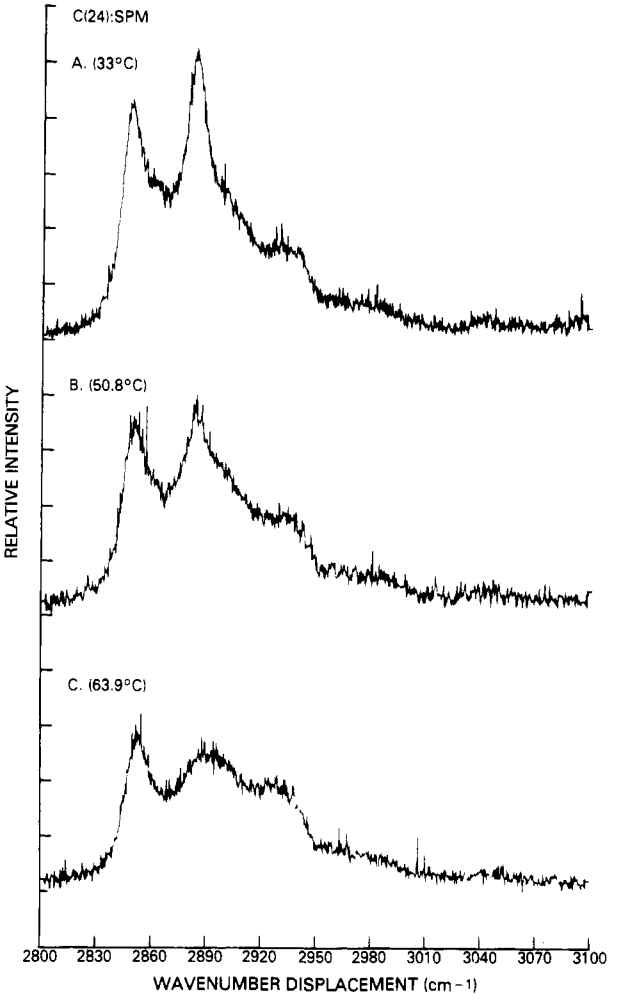

FIGURE 1: Raman spectra of the 2800–3100-cm^{-1} C–H stretching-mode region for aqueous dispersion of C(24):SPM (20% by weight) in (A) the gel II state at 33.0 °C, (B) the gel I state at 50.8 °C, and (C) the liquid-crystalline state at 63.9 °C.

Results and Discussion

Figure 1A depicts a typical Raman spectrum of a C(24):SPM dispersion recorded at 33 °C in the C–H stretching-mode region between 2800 and 3100 cm^{-1}. Three spectral features are particularly evident in this vibrationally congested region: the two relatively sharp bands at 2847 and 2882 cm^{-1}, attributed to the symmetric and asymmetric C–H stretching modes, respectively, for the coupled methylene groups constituting the hydrocarbon region of the phospholipid assembly

[1] Abbreviations: C(24):SPM, DL-*erythro*-*N*-lignoceroylsphingosylphosphocholine; C(18):C(10)PC, 1-stearoyl-2-caproyl-*sn*-glycero-3-phosphocholine; C(18):C(12)PC, 1-stearoyl-2-lauroyl-*sn*-glycero-3-phosphocholine; C(18):C(16)PC, 1-stearoyl-2-palmitoyl-*sn*-glycero-3-phosphocholine; diC(14)PC, 1,2-dimyristoyl-*sn*-glycero-3-phosphocholine; diC(16)PC, 1,2-dipalmitoyl-*sn*-glycero-3-phosphocholine; diC(18)PC, 1,2-distearoyl-*sn*-glycero-3-phosphocholine; diC(20)PC, 1,2-diarachidonoyl-*sn*-glycero-3-phosphocholine.

Table I: Raman Spectroscopic Data for Various Fully Hydrated Phospholipid Systems

phospholipid–H_2O system	temp (°C)	Raman peak-height intnsity ratio[a] $I(2932\ cm^{-1})/I(2882\ cm^{-1})$	Raman peak-height intnsity ratio[a] $I(2847\ cm^{-1})/I(2882\ cm^{-1})$	phase characteristics and references
diC(14)PC	13.8	0.45		T_m = 23.8 °C, lamellar gel phase[b]
	33.8	0.81		noninterdigitated liquid-crystalline phase[b]
diC(16)PC	31.3	0.42		T_m = 41.3 °C, lamellar gel phase[b]
	51.3	0.82		noninterdigitated lamellar liquid-crystalline phase[b]
diC(18)PC	43.5	0.39		T_m = 53.5 °C, lamellar gel phase[b]
	63.5	0.82		noninterdigitated lamellar liquid-crystalline phase[b]
diC(20)PC	55	0.38		T_m = 64.7 °C, lamellar gel phase[b]
	75	0.82		noninterdigitated lamellar liquid-crystalline phase[b]
C(18):C(12)PC	6.8	0.38	0.74	T_m = 16.8 °C, mixed interdigitated lamellar gel phase[c,d]
	27	0.78		liquid-crystalline phase with small degree of interdigitation[c,d]
C(18):C(16)PC	32	0.45	0.92	T_m = 42 °C, partially interdigitated lamellar gel phase[c,e]
C(24):SPM	38	0.31	0.76	$T_{m,1}$ = 48.5 °C, gel II phase (this work)
	49–53	0.42	0.91	$T_{m,2}$ = 54.5 °C, gel I phase (this work)
	64	0.78		liquid-crystalline phase (this work)

[a] The errors in the Raman peak-height intensity ratio are within 5% of listed values. [b] Huang et al., 1982. [c] Huang et al., 1983. [d] Hui et al., 1984. [e] Mason et al., 1981.

and a broad band centered approximately at 2932 cm^{-1}, assigned, in part, to a Fermi resonance component of the symmetric C–H stretching modes of the hydrocarbon chain terminal methyl groups. Although the Raman spectral 2900-cm^{-1} C–H stretching-mode spectra are extremely sensitive to both the intrachain conformational disorder and the lattice-packing characteristics of the hydrocarbon chains in the phospholipid assembly, the Raman peak-height intensity ratios [$I(2932\ cm^{-1})/I(2882\ cm^{-1})$ and $I(2847\ cm^{-1})/I(2882\ cm^{-1})$] are commonly used to monitor primarily the lateral chain–chain order/disorder rearrangements as the phospholipid assembly undergoes the endothermic gel → gel and gel → liquid-crystalline phase transitions (Huang et al., 1982, 1983).

The temperature profile derived from the Raman peak-height intensity ratio, $I(2932\ cm^{-1})/I(2882\ cm^{-1})$, for C(24):SPM dispersions, shown in Figure 2, displays two clearly discernible order/disorder transitions centered at 48.5 and 54.5 °C. Below the onset temperature of the lower temperature order/disorder transition, the Raman peak-height intensity ratio of $I(2932\ cm^{-1})/I(2882\ cm^{-1})$ is relatively insensitive to temperature, averaging about 0.31 (Table I). This ratio is significantly smaller than the corresponding value observed for members of the homologous diC(14)PC to diC(20)PC series of saturated, symmetric phosphatidylcholine (Table I). The intensity ratios for these systems, which are in the gel state, vary from 0.45 to 0.38 as the chain lengths increase through the series (Table I). Since the peak-height intensity ratio of $I(2932\ cm^{-1})/I(2882\ cm^{-1})$ is indicative of both lattice disorder and intrachain conformational disorder of the lipid hydrocarbon chains, a smaller value of the ratio for C(24):SPM dispersions at temperatures below the first order/disorder transition at 48.5 °C implies that the hydrocarbon chains of C(24):SPM in the lipid lamellae are more highly ordered below this temperature than are saturated symmetric lamellar diC(16) and diC(18) phosphatidylcholines in the gel state. Various possible chain-packing arrangements for highly asymmetric phospholipid molecules in gel-state lamellae have been discussed in detail previously (Hui et al., 1984; Huang et al., 1983). Since the full length of the all-trans C(24) hydrocarbon chain is just about twice as long as the all-trans C–C segment of sphingosine base linked to the chain bend at the trans double bond extending from the C6 atom to the methyl terminal C18 atom and since the chain–chain interactions in the gel state C(24):SPM bilayer are very strong relative to those in gel-state diC(16)PC or diC(18)PC lamellae, the most likely chain-packing arrangement for C(24):SPM

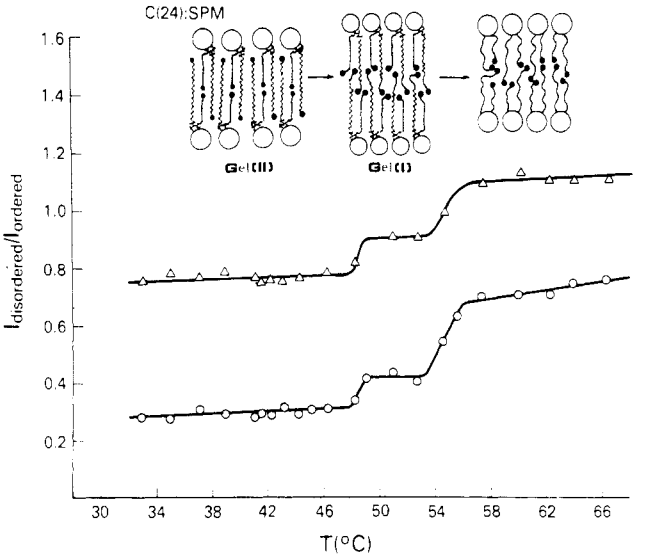

FIGURE 2: Temperature profiles for C(24):SPM dispersion in excess water. The Raman spectral peak-height intensity ratios $I(2935\ cm^{-1})/I(2882\ cm^{-1})$ (○) and $I(2847\ cm^{-1})/I(2882\ cm^{-1})$ (△) were used as indices for characterizing the structures and phase transitions of the hydrocarbon region of the lipid assembly. Proposed models depicting the molecular packing arrangement of fully hydrated C(24):SPM within the three phases are diagramatically represented above each region. In the gel I state, the zig-zag planes of the hydrocarbon chains are likely to undergo axial rotational motions.

in the bilayer at temperatures below the lower transition is one in which the highly asymmetric C(24):SPM molecules form a mixed interdigitated bilayer. In this model, the long hydrocarbon chain is interdigitated fully across the entire hydrocarbon width of the bilayer, while the short chain, which is about half as long as the other chain, packs end to end with the short chain of another lipid molecule in the opposing bilayer leaflet (McIntosh et al., 1984; Hui et al., 1984).

The value obtained for $I(2932\ cm^{-1})/I(2882\ cm^{-1})$ in the temperature region (49–53 °C) between the two discernible order/disorder changes is 0.42 (Figure 1B and 2), which indicates that the hydrocarbon chains of C(24):SPM have become progressively more disordered. However, a Raman spectral peak-height intensity ratio of $I(2932\ cm^{-1})/I(2882\ cm^{-1})$ equal to 0.82 is generally observed for saturated symmetric-chain phosphatidylcholines, such as diC(16) and diC(18) phosphatidylcholines, in the liquid-crystalline state (Table I). The intensity ratio of 0.42 observed for C(24):SPM dis-

persions implies that the hydrocarbon chains of this lamellar sphingomyelin in the temperature region between the two order/disorder transitions are much more ordered than the acyl chains of saturated symmetric lamellar diC(16) or diC(18) phosphatidylcholines in the liquid-crystalline state; furthermore, the magnitude of the Raman intensity ratio (0.42) is comparable with that of gel-state diC(14)PC (0.45), diC(16)PC (0.42), and C(18):C(16)PC (0.45) at the same reduced temperature (Table I). C(24):SPM dispersions can therefore, be considered as in the gel phase within the temperature range between the two transitions; hence, the lower order/disorder transition can be ascribed to a gel II to gel I phase transition.

As the C(24):SPM dispersion is heated above 53 °C, the Raman peak-height intensity ratio $I(2932\ cm^{-1})/I(2882\ cm^{-1})$ increases abruptly and reaches a value of 0.72 at 57 °C (Figures 1C and 2). Above 57 °C, however, the ratio increases gradually with increasing temperature (Figure 2). The values of the Raman peak-height intensity ratio $I(2932\ cm^{-1})/I(2882\ cm^{-1})$ at various temperatures obtained for C(24):SPM dispersions above 57 °C are similar to those obtained for saturated asymmetric C(18):C(12)PCs in the liquid-crystalline state recorded at corresponding reduced temperatures (Table I). On the basis of the temperature dependence of the Raman intensity ratio of $I(2932\ cm^{-1})/I(2882\ cm^{-1})$, as shown in Figure 2, we conclude that although the lower temperature order/disorder transition corresponds to a gel II → gel I phase transition, the higher temperature order/disorder transition appears to correspond to a gel I → liquid-crystalline phase transition.

The temperature dependence of the relative intensities of the methylene symmetric and asymmetric C–H stretching modes, at approximately 2847 and 2882 cm^{-1}, respectively, for C(24):SPM dispersions is also shown in Figure 2. The relative intensities of these modes reflect lateral chain–chain interactions in phospholipid assemblies that are perhaps less perturbed by intrachain conformational changes (Snyder et al., 1978; Levin, 1984). The temperature profile based upon the relative intensities of the 2847- and 2882-cm^{-1} features is parallel to that derived for the $I(2932\ cm^{-1})/I(2882\ cm^{-1})$ intensity ratio and also clearly shows two discontinuities. The value of $I(2847\ cm^{-1})/I(2882\ cm^{-1})$ is 0.76 at 10 °C below the onset temperature of the first transition (48 °C); this value may be compared favorably with a value of 0.74 observed for saturated asymmetric C(18):C(12)PC dispersions measured at 10 °C below the main phase-transition temperature (Table I), suggesting that the lateral chain–chain interactions of lamellar C(24):SPM in the gel II state are similar to those of C(18):C(12)PC in the mixed interdigitated bilayer. Thus, from the Raman spectroscopic indices, $I(2847\ cm^{-1})/I(2882\ cm^{-1})$ and $I(2932\ cm^{-1})/I(2882\ cm^{-1})$, we conclude that at temperatures below 48 °C the hydrocarbon chains of C(24):SPM in a dispersion, in excess water, are highly ordered; furthermore, these hydrocarbon chains probably adopt a mixed interdigitated chain packing as shown diagrammatically in Figure 2.

At temperatures between the two order/disorder transitions, we have already presented spectroscopic evidence, based on the $I(2932\ cm^{-1})/I(2882\ cm^{-1})$ Raman peak-height intensity ratio, that the hydrocarbon chains of C(24):SPM dispersions are much more ordered than those observed for saturated symmetric diC(16) and diC(18) phosphatidylchlolines in the liquid-crystalline phase. The relative Raman intensity ratio of $I(2847\ cm^{-1})/I(2882\ cm^{-1})$ for C(24):SPM in the temperature region between the two order/disorder changes is 0.91 (Figure 2), in close agreement to that of 0.92 obtained for

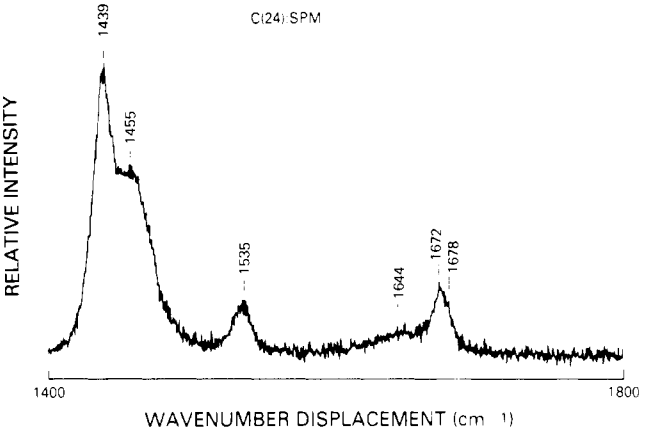

FIGURE 3: Raman spectrum of C(24):SPM dispersions in the 1400–1800-cm^{-1} region. Temperature was 6.4 °C.

slightly asymmetric C(18):C(16)PCs in the gel state at about 10 °C below T_m (Table I). Thus, the magnitude of the lateral chain–chain interactions for C(24):SPM dispersions in the temperature region between 49 and 53 °C is comparable to that of gel-state C(18):C(16)PC dispersions at approximately 10 °C below T_m. For the C(18):C(16)PC system, the geometrically defined central region of the gel-state bilayer is assumed to be partially interdigitated; moreover, the lateral chain–chain packing in this central region is considered to be significantly perturbed by the bulky methyl groups at the terminal ends of the inequivalent *sn*-1 and *sn*-2 acyl chains (Mason et al., 1981). In fact, such partial chain interdigitation also may be occurred in the gel-state bilayer of diC(14)PC or diC(16)PC, due to the inequivalent chain configurations of diacylphosphatidylcholines at the *sn*-1 and *sn*-2 positions (Mason & Huang, 1981; Huang & Levin, 1983).

The suggested hydrocarbon chain packing modes of C(24):SPM in bilayers that exist within the three different phases are diagramatically represented in Figure 2 above each of the representative temperature regions. The most ordered phase in the low-temperature region (<48 °C) is proposed to be a mixed interdigitated or gel II phase in which the shorter C–C segment of the sphingosine base is packed end to end with the C–C segment of a sphingosine base of another C(24):SPM in the opposing bilayer leaflet, while the longer C(24) hydrocarbon chain from the two leaflets spans the entire hydrocarbon width of the bilayers; the intermediate phase is a gel I phase in which two leaflets are partially interdigitated in the center of the bilayer. The high-temperature phase is a highly disordered liquid-crystalline phase.

Raman spectral features in the methylene deformation region (1400–1500 cm^{-1}) are sensitive to the two-dimensional chain packing for the hydrocarbon chains of phospholipid assemblies in the gel state (Levin, 1984; Huang et al., 1984). A typical Raman spectrum of the mixed interdigitated gel phase (6.4 °C) of C(24):SPM dispersions in the CH_2 deformation region is depicted in Figure 3. A methylene deformation doublet is clearly observed with a strong narrow band at 1439 cm^{-1} and a high-frequency shoulder (~1455 cm^{-1}); however, this region fails to reveal the ~1420-cm^{-1} vibrational feature characteristic of hydrocarbon chains packed in orthorhombic subcells (Boerio & Koenig, 1970). The two-dimensional chain packing of a cerebroside species, β-D-galactosyl-*N*-(D-2-hydroxyoctadecanoyl)-D-dihydrosphingosine, in crystals has been reported by Pascher & Sundell (1977). Their X-ray crystallographic data demonstrate that the plane of the *N*-acyl chain zig-zag carbon–carbon backbone is nearly perpendicular to the plane of the sphingosine long-chain zig

zag carbon–carbon backbone. This nearly perpendicular chain-plane packing is designated as the HS2 type, which can be considered as a hybrid of several simpler subcells. None of the simpler HS2 subcells, however, can be assigned as an orthorhombic lattice, since one of the chain planes of the four corners of the simplest two-dimensional rectangular lattice always has an orientation that is nearly perpendicular to that exhibited by the hydrocarbon chains in the other three corners (Pascher & Sundell, 1977; Abrahamsson et al., 1978). The fact that the Raman spectrum in the methylene deformation region does not reveal the $\sim$1420-cm^{-1} vibrational band as shown in Figure 3 suggests strongly that the hydrocarbon chains of C(24):SPM in the mixed interdigitated gel state do not pack with orthorhombic symmetry in the two-dimensional lattice (Huang et al., 1984). This result is clearly consistent with the notion that the hydrocarbon chains of mixed interdigitated C(24):SPM are likely packed in simpler hybrid subcells. However, the Raman spectrum does not prove that the two-dimensional hybrid chain packing observed for cerebroside in crystals can be extrapolated directly to the hydrocarbon chain packing for C(24):SPM in the mixed interdigitated gel state. Resolving this issue unequivocally requires more detailed studies utilizing another physical technique, such as X-ray diffraction.

The 1500–1680-cm^{-1} region, shown in Figure 3, encompasses the amide II, amide I, and the trans double bond spectral intervals. The prominent 1672-cm^{-1} feature is assigned to the trans double bond between C4 and C5 of the sphingosine moiety, while the broad feature centered approximately at 1644 cm^{-1} reflects the amide I band associated with the amide linkage between the acyl chain and the amino group of sphingosine base (Bunow & Levin, 1980). The amide II band, reflecting a mixed C–N stretching and an N–H in-plane bending mode, is observed at 1535 cm^{-1}.

In summary, the present Raman spectral studies show two thermal transitions centered at 48.5 and 54.5 °C in multilamellar dispersions of racemic C(24):SPM–H_2O systems that have been incubated at 0 °C for an extended period. The lower temperature transition appears to correspond to a transformation from a mixed interdigitated gel II state to a nearly interdigitated gel I state. The higher temperature transition corresponds to a gel I $\rightarrow$ liquid-crystalline phase transition. It should be emphasized that the Raman data were obtained from lipid samples that had been incubated for a prolonged period at 0 °C. Different temperature profiles were observed if the C(24):SPM–H_2O system was annealed at 0 °C for much shorter periods of time, indicating that the thermal behavior of the system is history dependent (data not shown). Clearly, because of the hysteresis effects inherent in asymmetric chain systems, other physical studies are needed to substantiate the structural characteristics of the three phases for C(24):SPM in excess water in the temperature range from 30 to 65 °C.

In contrast to most glycerol-based lipids, the sphingomyelin found in biological membranes exhibits the same type of hydrocarbon chain length asymmetry as does the synthetic sphingomyelin discussed in this paper. The mixed interdigitation that occurs in bilayers formed from this sphingomyelin suggests the possibility that such interdigitation might also occur under certain conditions between sphingomyelin molecules packed in the opposite faces of a biological membrane. Indeed, if mixed interdigitation does occur in biological membranes, the penetration of long asymmetric lipid hydrocarbon chains across the entire hydrocarbon width of the bilayer affords a transmembrane linkage that could play an important role in the transmission of information across these membranes.

References

Abrahamsson, S., Dahlen, B., Lofgren, H., & Pascher, I. (1978) *Prog. Chem. Fats Other Lipids 16*, 125–143.

Barenholz, Y., & Thompson, T. E. (1980) *Biochim. Biophys. Acta 604*, 129–158.

Barenholz, Y., Suurkuusk, J., Mountcastle, D., Thompson, T. E., & Biltonen, R. L. (1976) *Biochemistry 15*, 2441–2447.

Boerio, F. S., & Koenig, J. L. (1970) *J. Chem. Phys. 52*, 3425–3431.

Bunow, M. R., & Levin, I. W. (1980) *Biophys. J. 32*, 1007–1022.

Huang, C., & Levin, I. W. (1983) *J. Phys. Chem. 87*, 1509–1513.

Huang, C., Lapides, J. R., & Levin, I. W. (1982) *J. Am. Chem. Soc. 104*, 5926–5930.

Huang, C., Mason, J. T., & Levin, I. W. (1983) *Biochemistry 22*, 2775–2780.

Huang, C., Mason, J. T., Stephenson, F. A., & Levin, I. W. (1984) *J. Phys. Chem. 88*, 6454–6458.

Hui, S. W., Mason, J. T., & Huang, C. (1984) *Biochemistry 23*, 5570–5577.

Levin, I. W. (1984) *Adv. Infrared Raman Spectrosc. 11*, 1–48.

Mason, J. T., & Huang, C. (1981) *Lipids 16*, 604–608.

Mason, J. T., Huang, C., & Biltonen, R. L. (1981) *Biochemistry 20*, 6086–6092.

McIntosh, T. J., Simon, S. A., Ellington, J. C., & Porter, N. A. (1984) *Biochemistry 23*, 4038–4044.

Pascher, I., & Sundell, S. (1977) *Chem. Phys. Lipids 20*, 175–191.

Snyder, R. G., Hsu, S. L., & Krimm, S. (1978) *Spectrochim. Acta, Part A 34A*, 395–406.